

FRACTURE LIKELIHOOD ANALYSIS USING TRIPLE COMBO LOG DATA IN THE STACKED CARBONATE PLAY OF MADISON COUNTY

Courtney Beck, Anna Khadeeva, Bhaskar Sarmah, and Andrew Whitsett,
Halliburton

Trey Kimbell,
Burk Royalty

INTRODUCTION

The presence of natural fractures is important for understanding production in many carbonate plays globally. Natural fractures increase reservoir connectivity and lead to increased hydrocarbon recovery, particularly in tight carbonate plays, where faulting is the dominant structural feature. Resistivity image logs provide information about fracture distribution and orientation around the wellbore. However, traditional methods of natural fracture detection are often costly and only provide information directly at the wellbore. Running an image log can also be difficult to execute, depending on borehole conditions. This study presents an indirect method of detecting natural fractures using openhole logs and seismic data.

The fracture indicator curve developed here was calibrated to two resistivity image logs on wells in the stacked carbonate play of Madison County, East Texas, and applied to 29 wells across the asset. Three-dimensional (3D) seismic attributes were analyzed to infer the presence of natural fractures away from the wellbores. Normalized production data from vertical wells in the area were compared to fault and fracture maps and supported the hypothesis that natural fracture detection is important for the stacked carbonate play in East Texas.

GEOLOGIC SETTING

Oil and gas production in East Texas historically came from the Woodbine and Sub-Clarksville sand formations (Bruno et al., 1991) and, beginning in the 1960s, from stacked carbonates below clastic units (Pampe, 1963). The stacked pay consists of the Buda, Georgetown, Edwards, and Glen Rose Cretaceous carbonate formations, at depths of 9,200 to 12,600 ft. Operators drilling vertical wells typically perforate and complete all four carbonate layers; but, in recent years, the Buda/Georgetown has become the target for horizontal wells in the area. This study mainly focuses on fractures in the Buda/Georgetown interval.

The carbonate layers in East Texas are separated by shale and shaly limestone and represent a depositional environment that alternated between carbonate and siliciclastic dominated (Dennen and Hackley, 2012). The deepest of the carbonate layers, the Glen Rose, was deposited during the Aptian-Albian in a highstand carbonate platform setting (Dennen and Hackley, 2012). The Glen Rose is more than 500-ft thick and divided into five zones based on gamma ray cutoffs—the Glen Rose A through E (Figure 1). The Glen Rose is an argillaceous carbonate formation, with higher clay content in the C through E layers. Interfingering with the top of the Glen Rose is the Paluxy, a calcareous shale representing a change from fluvial-deltaic clastic deposition to the purely marine depositional environment of the Edwards formation (Dennen and Hackley, 2012; Anderson, 1989).

The Edwards formation overlies the Paluxy and is a fractured argillaceous limestone divided into two sections—the Edwards A and B. Both sections can be identified on well logs and seismic. In this area, the Edwards B is a cleaner limestone with a relatively constant thickness. The carbonate-rich upper section of the Edwards A pinches out toward the southeast into a more clay-rich zone. The Edwards A is overlain by the Kiamichi, a series of calcareous shales and shaly limestones. In the study area, the Kiamichi thickens

to the southeast, ranging in thickness from 30 ft in the northwest to over 200 ft in the southeast. The underlying Edwards A formation thins as the Kiamichi thickens (Pampe, 1963).

The Buda and Georgetown are clean platform carbonates separated by a thin regionally extensive shale, the Del Rio. Both the Buda and Georgetown formations have low matrix porosity and depend on natural fractures for secondary porosity. Locating natural fracture swarms in this area is crucial to drilling successful wells but has proven to be difficult (Albrecht et al., 2015). Operators in this area are currently drilling and hydraulically fracturing horizontal wells in the Buda/Georgetown section in attempts to intersect natural fracture swarms, with promising initial production results.

METHODS AND WORKFLOW

Interpretation of Geologic Data

The dataset for this area comprised a 98-square mile 3D seismic survey and 43 wells with triple combo logs, five of which had sonic data (Figure 2). Formation tops for the Buda, Georgetown, Kiamichi, Edwards A and B, Paluxy, and Glen Rose A through E were interpreted. The wells with sonic data were used to tie the formation tops to the seismic. The following horizons were interpreted: Buda, Edwards A and B, and Glen Rose A, B, and E (Figure 1). The horizons were converted to depth and used along with formation tops in a structural framework to create a 3D grid with 13 intervals and 10.5 million cells. The grid cells were 400 × 400 ft, with an average cell thickness of 3.5 ft.

EUR Calculation and Production Normalization

Production information was provided for 35 vertical wells in the study area (Figure 3). The information included complete daily oil, gas, and water production for each well. Production analysis was complicated because of comingled production from the Buda, Georgetown, Edwards, and Glen Rose intervals. Not every well was completed in each of the four intervals of interest, but each well had at least three intervals completed. No production logs were available to quantify production per interval.

Variance in the production data made estimated ultimate recovery (EUR) calculations inaccurate for certain wells. Instead, 90-day accumulations were compared for oil, gas, barrel of oil equivalent (BOE), and water. Two wells were eliminated from the dataset because they did not meet the minimum requirement of 250 days of production. The 90-day oil and gas barrel of oil equivalent (BOE) production accumulations were used as a proxy for EUR because it was not possible to complete EUR analysis for every well. While certain wells were still producing a significant amount after 250 days, production levels had declined sufficiently for a clear separation to exist between the wells.

Petrophysical Analysis and Fracture Indicator Curve Computation

Wireline measurements, such as density, resistivity, caliper, and gamma ray, are often good indicators of the presence of natural fractures. Resistivity and high-frequency acoustic images in a borehole can provide a detailed picture of the fracture system that traverses the well path. In the absence of an image log, indirect methods can be applied to identify natural fractures using triple combo log data. The vertical resolution of openhole logs is much bigger than a possible fracture aperture, but with the presence of multiple fractures and/or associated borehole breakup, openhole logs can be helpful for identifying natural fractures.

In this study, a fracture indicator curve was developed using the density log response as an indicator of the presence of natural fractures. The derivative of the density was calculated to highlight changes in density values, particularly a sudden drop in density. From the image logs in the area, it has been observed that the fracture density across the clay-rich sections tends to be low to nonexistent. To eliminate the effect of lithological changes, particularly in the clay-rich sections, a gamma ray cutoff was applied.

The fracture indicator curve was calibrated to image log interpretation on two wells with both borehole image and triple combo log data. A reasonable correlation was observed between the fractures interpreted from the image log and those predicted from the fracture indicator curve. A further adjustment was applied to the model, with the lower value of the derivative matched to the image log interpreted fractures, and a good calibration was established.

Figure 4 compares the predicted fractures and the interpreted fractures from the image log data. The histograms on the right side of the fracture track indicate the predicted fractures. The fracture density curves representing different fracture types, such as open conductive, partial conductive fractures, etc., are also presented in the fracture track, increasing from left to right. Some borehole breakups along the fracture planes can be observed in the image track (black patches). Density measurement is acquired using a pad extending to the borehole wall from the tool. These breakups of the borehole wall along the fracture plane cause a decrease in the density value, which is used in the fracture indicator model to identify fractures.

Drilling induced fractures are also predicted using this methodology (Figure 5). Drilling induced fractures are generally parallel to the borehole. They appear as two nearly parallel dark curves that are 180° apart in a resistivity image log.

In addition to the fracture indicator curve, standard petrophysical properties, such as mineral volumes, fluid saturations, and porosity, were calculated. A pay cutoff was established that set maximum values for water saturation and clay volume and minimum values for porosity. However, the pay cutoff did not show a robust correlation with actual production data. Some of the highest producing wells in the area did not appear to be in a pay zone when considering only petrophysical properties across the entire stacked carbonate interval. Analogous to many carbonate plays around the world, the main driver of production in the study area appeared to be natural fracture networks or secondary interconnected porosity networks.

Post-stack Seismic Attributes

As discussed previously, it is expected that natural fractures will occur in brittle carbonates and will not propagate into ductile clays. Also, more fractures are expected to occur near fault zones as fractures precede the faulting and define the planes of weakness along which the fault breaks (Antonellini and Aydin, 1995; Shipton and Cowie, 2003). In this study, P-impedance inversion and discontinuity attributes showed the best correlation to fracture and production prediction.

P-impedance can sometimes be used to determine rock lithology if the velocity and density contrast of the rock interfaces is relatively large and the lithology model is known from petrophysical logs. In the current study, P-impedance seismic volume was compared to lithology logs, and an inverse correlation between clay volume and impedance was observed (Figure 6). Thus, it was possible to determine which rock layers were likely to be fractured.

Discontinuity is a structural attribute that was used for fault mapping in the study area (Figure 7). Using the location of faults interpreted from the discontinuity volume, it was possible to determine where fractures had a higher probability of occurring.

Blocking Seismic Properties and Fracture Indicator Curve to 3D Grid

To perform statistical comparisons between the fracture indicator curve, seismic attributes, and petrophysics, the log and seismic properties were scaled, or blocked, to the 3D grid (Figure 8). Blocking the seismic and log data to the 3D grid creates a single dataset that has the same vertical resolution as the 3D grid. The cells in the 3D grid are 3.5 ft in the vertical direction. The blocking process for logs averages the values of a given log across each grid cell, creating one value per cell per log property. For seismic attributes, such as discontinuity and P-impedance, the blocking process calculates the arithmetic average of all seismic attribute values that fall within a particular grid cell and assigns the average value

to the center of the cell. The fracture indicator curve has discrete values, with a value of 0 indicating unfractured rock and a value of 1 indicating fractured rock. The lithotype definition function codes every data point in the blocked dataset as either “unfractured” or “fractured” based on the data from the fracture indicator curve. Dividing the dataset into unfractured and fractured categories allows comparison of the properties and identification of trends unique to each group.

RESULTS AND DISCUSSION

Comparison of Discontinuity to Fracture Indicator Curve

The discontinuity attribute is a good visual indicator of faulted areas (Figure 9). However, it does not directly correlate to the fracture indicator curve or an image log. Figure 10 shows a well with a fracture indicator curve that was calibrated to an image log located approximately 2,600 ft outside the edge of the seismic survey. Although no clear fault planes can be observed in the discontinuity volume, fractures are still present in the well. A possible explanation for the presence of fractures in the well close to a relatively clean discontinuity volume is that seismic is only available away from the well, and the entire 360° view is not available around the wellbore to determine if any faulting exists on other sides. Also, the presence of fractures does not have to be associated with the proximity to faults because fracturing precedes faulting, and fracture zones do not necessarily develop into fault planes. However, faults always have some amount of fracturing surrounding them. Mapping faults and determining the distance to which the fractures associated with faults propagate helps determine the most probable fractured areas first and decreases uncertainty in finding better drilling locations.

Correlation Between Production and Proximity to Faulted Zones

Ninety day oil and gas (BOE) production data were overlain on a discontinuity slice through the Buda to determine how faulting affects well performance (Figure 11). In the production bubble map, the larger circles represent higher production. Many wells with high production are located in the northern part of the study area, where most of the faulting (black or grey linear features) occurs. It also can be noted that wells with lower production are situated directly on top of the faults. This trend can be explained by the loss of fluids through the faulted zones and, thus, lower production numbers. From this observation, it can be inferred that better production can be achieved by placing wells near the faulted zones. However, caution should be used when selecting drilling locations, as drilling directly through a fault can cause poor well performance.

Comparison of P-Impedance to Clay Volume

Fractures are sparse or absent in the clay-rich zones (greater than 25% clay volume) in this area. This was directly measured on one of the wells for which an image log and clay volume analysis existed. The same observation applied to other wells with the fracture indicator curve, so it was inferred that clay-rich sections throughout this area generally have few to no fractures present. A direct comparison of clay volume to the P-impedance seismic data showed two distinct data clusters (Figure 12). A group of high clay values, greater than 45%, exists between P-impedance values of 24,000 to 34,000 ft/s × g/cc. A second group of values with a generally lower clay volume, below 50%, exists between 34,000 to 54,000 ft/s × g/cc. From this, it is expected that lower P-impedance values, between 24,000 to 34,000 ft/s × g/cc, indicate high clay volume. This relationship between clay volume and P-impedance can be used as a proxy to indicate where clay-rich zones are present in the study area. Natural fractures are not likely to occur in clay-rich zones, so these areas should be avoided.

CONCLUSIONS

Identifying natural fracture swarms and strategically placing wells in such areas is important for the East Texas stacked carbonate play. This study presents a workflow to identify natural fractures using log and seismic data. A good correlation between resistivity image log data and triple combo log data was established, and the resulting fracture indicator curve was used to identify areas having a high probability of natural fractures. Post-stack seismic attributes, such as discontinuity and P-impedance, were also

useful for predicting the locations of natural fractures. Discontinuity provided a good visual indicator of faulting and presumed fractured zones. A positive correlation between high producing wells and faulted zones was observed in this dataset. Additionally, a relationship between high clay volume and low P-impedance was established. This relationship can be used to predict zones that are not likely to have natural fractures, which should not be considered as drilling targets.

The workflow established here is a low-cost solution to help reduce the number of necessary image logs for successful reservoir characterization and understanding of natural fracture trends. This information can be used to choose optimal surface locations, stratigraphic targets, and perforations for horizontal and vertical wells in the East Texas stacked carbonate play.

REFERENCES

Albrecht, T., Kerchner, S., Brooks, S., Kolstad, E., Willms, T., Klein, J., and Stemler, D., 2015, Innovation is key to finding new oil in an old sandbox – East Texas stacked play: Unconventional Resources Technology Conference, San Antonio, TX. DOI 10.15530/urtec-2015-2153354.

Anderson, L.M., 1989, Stratigraphy of the Fredericksburg Group, East Texas Basin: Baylor Geological Studies Bulletin No. 47, p. 1-38.

Antonellini, M. and Aydin, A., 1995, Effect of faulting on fluid flow: geometry and spatial distribution: AAPG Bulletin 79 (5): 642-671.

Bruno, L., Roy, D.L., Grinsfelder, G.S. and Lomando, A.J., 1991, Alabama Ferry Field—USA East Texas Basin-Texas: American Association of Petroleum Geologists Special Publication 7 Stratigraphic Traps II, 27 p.

Dennen, K.O., and Hackley, P.C., 2012, Definition of greater Gulf basin Cretaceous shale gas assessment unit, United States Gulf of Mexico basin onshore and state waters: American Association of Petroleum Geologists Annual Convention and Exhibition, Houston, TX. Search and Discovery Article #10426.

Pampe, C.F., 1963, The Fort Trinidad “Glen Rose” Field: South Texas Geological Society Bulletin, 11 p.

Shipton, Z.K. and Cowie, P.A., 2003, A conceptual model for the origin of fault damage zone structures in high-porosity sandstones: Journal of Structural Geology 25, 333-344.

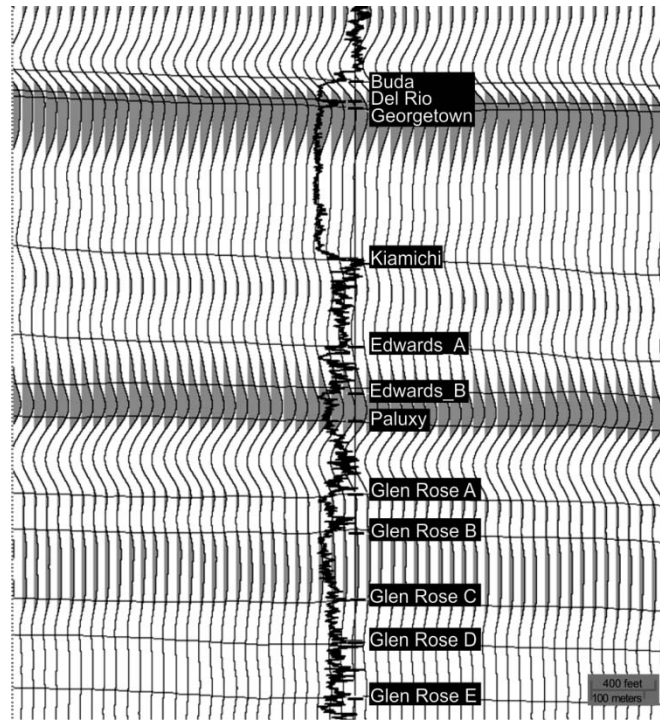


Figure 1 - Type curve (gamma ray) and seismic.

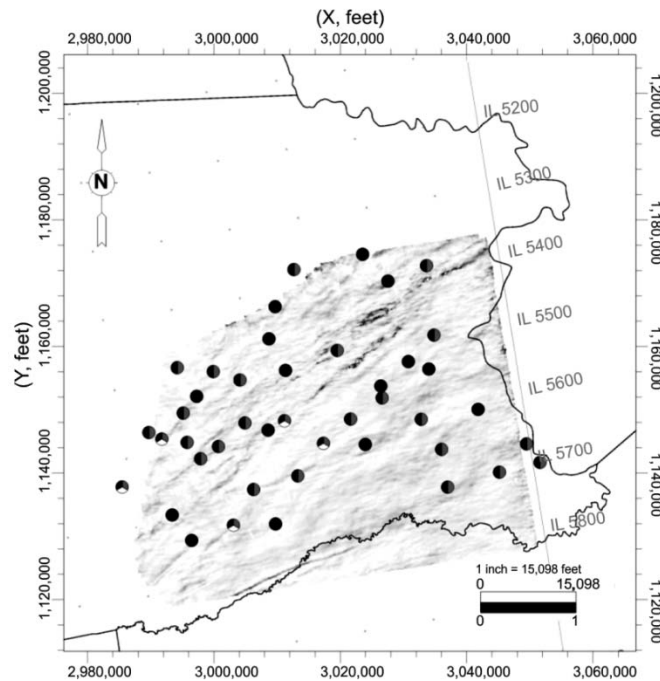


Figure 2 - Map of wells used in structural framework. Each pie chart represents a well location, and the colors of the pie chart indicate which log data were present at each well. Black represents triple combo, grey represents fracture indicator curve, and white represents sonic data.

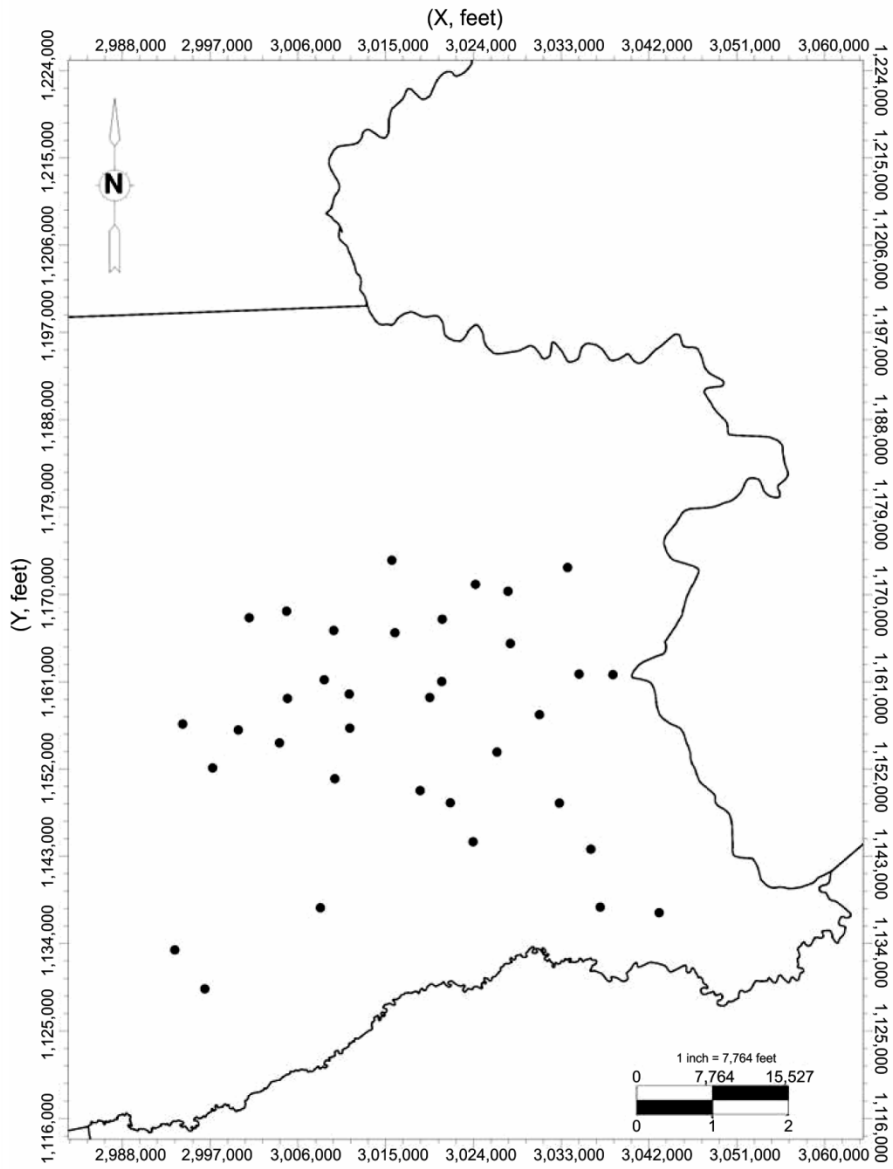


Figure 3 - Location of wells used in production analysis.

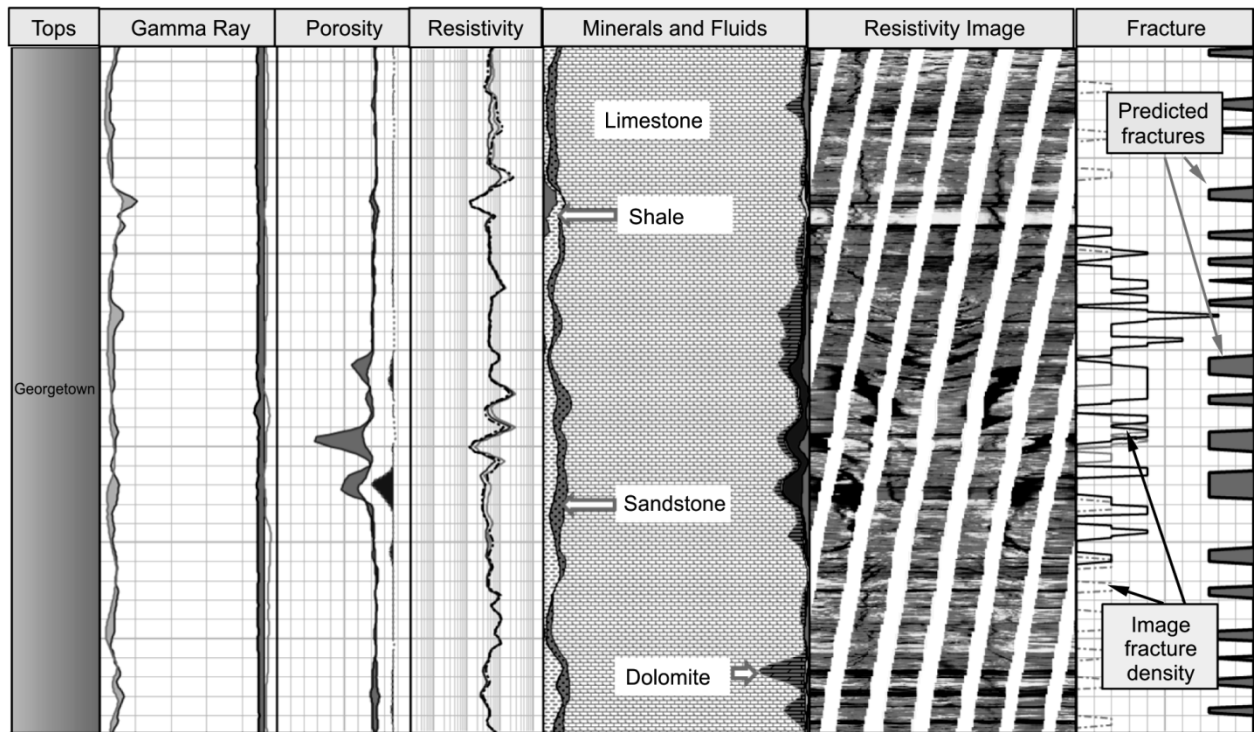


Figure 4 - A comparison between a predicted fracture and the natural conductive fracture density curves is shown in the right-hand track. The second track from right shows a resistivity-based image log. The mineral and fluid volumetric track shows the presence of fairly clean limestone in the section.

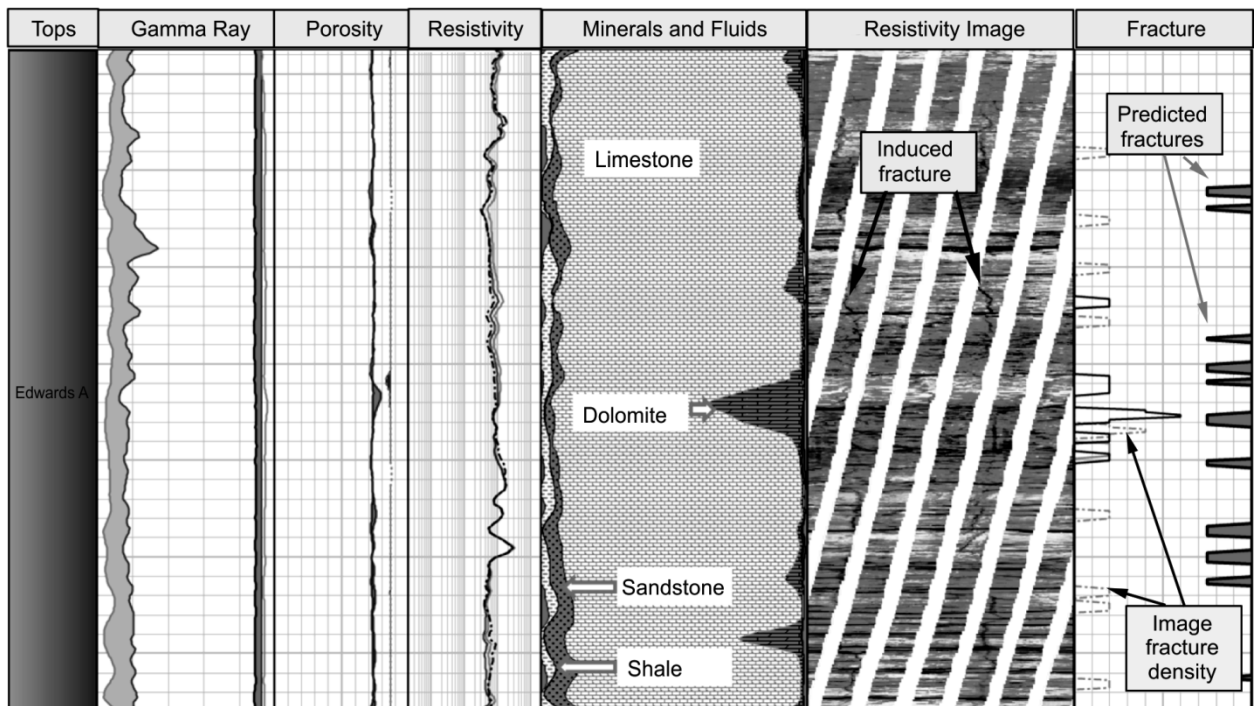


Figure 5 - A comparison between a predicted fracture and image-interpreted induced fracture is shown in the right-hand track. Induced fracture impressions can be observed in the resistivity image track.

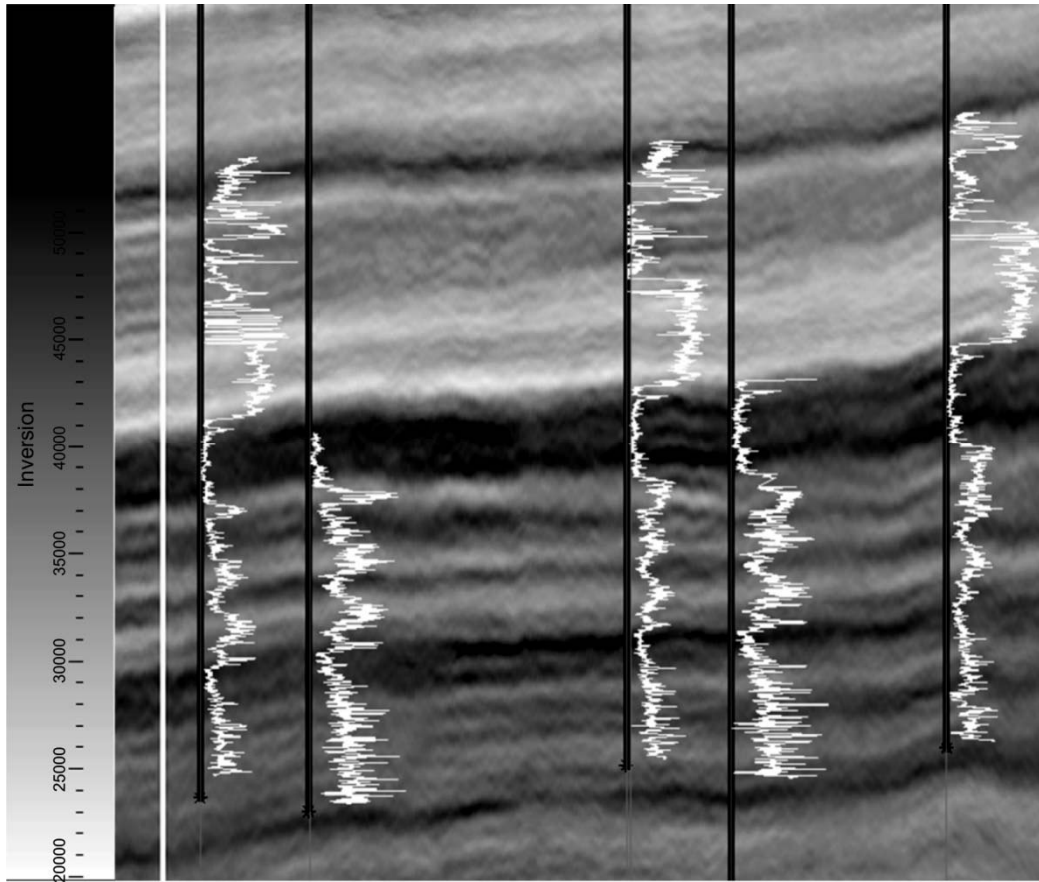


Figure 6 - Clay volume logs with seismic P-impedance volume in the background. Lighter colors represent lower values of P-impedance, which correspond to higher clay volume in logs.

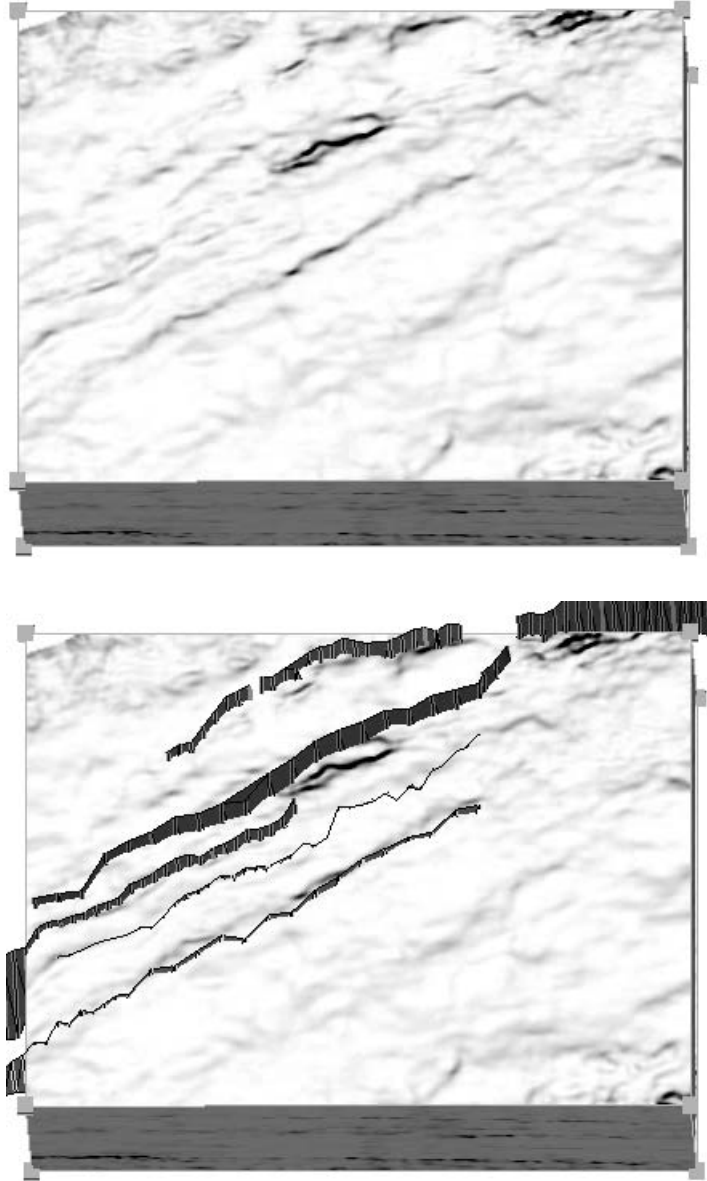


Figure 7 - Discontinuity volume showing potential faults as black and dark grey lines (top) and the same volume displaying interpreted faults (bottom).

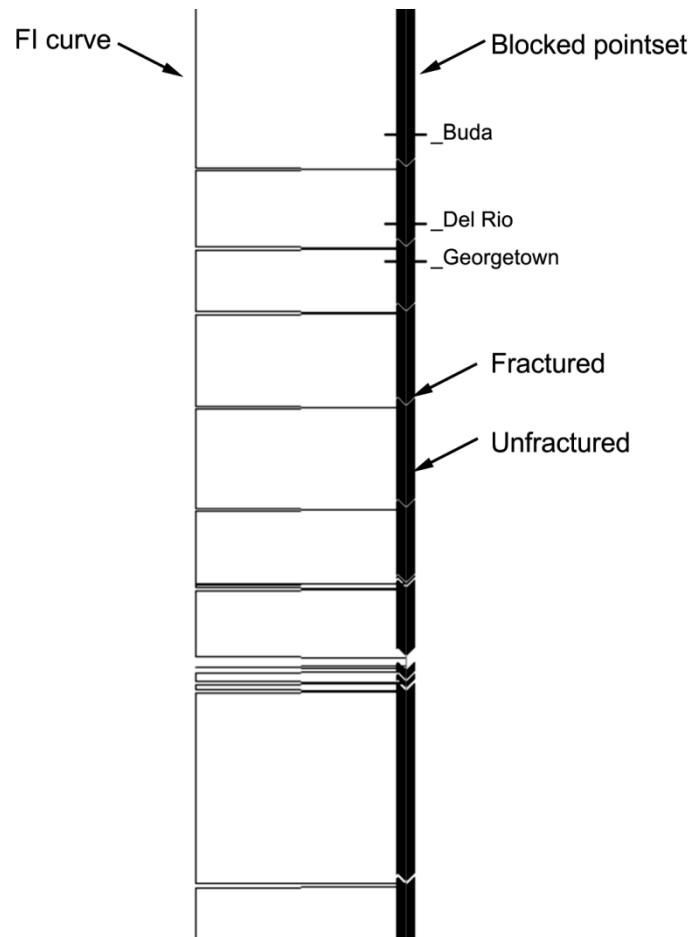


Figure 8 - Example of blocked dataset. In the pointset, the black data points represent unfractured rock and the white data points represent fractured rock.

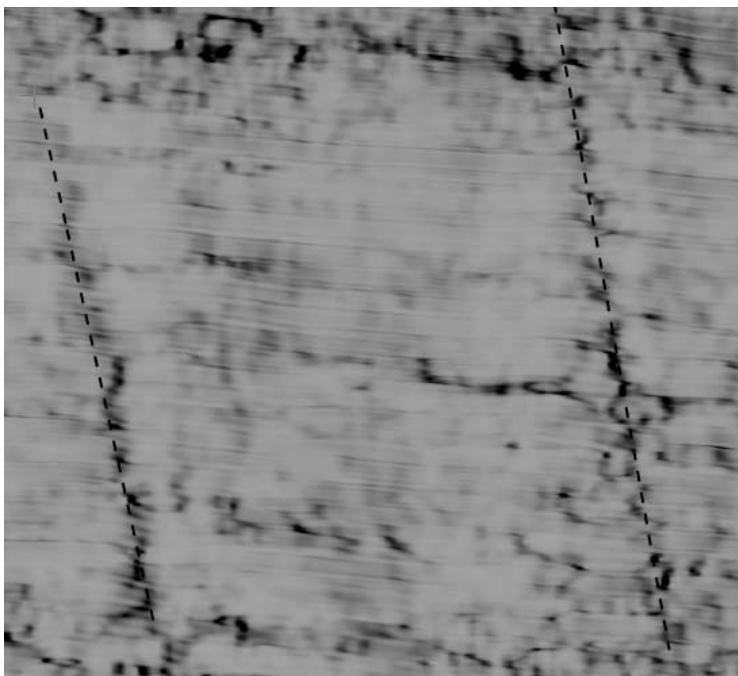


Figure 9 - Fault interpretation on discontinuity volume, with dashed black lines representing fault planes.

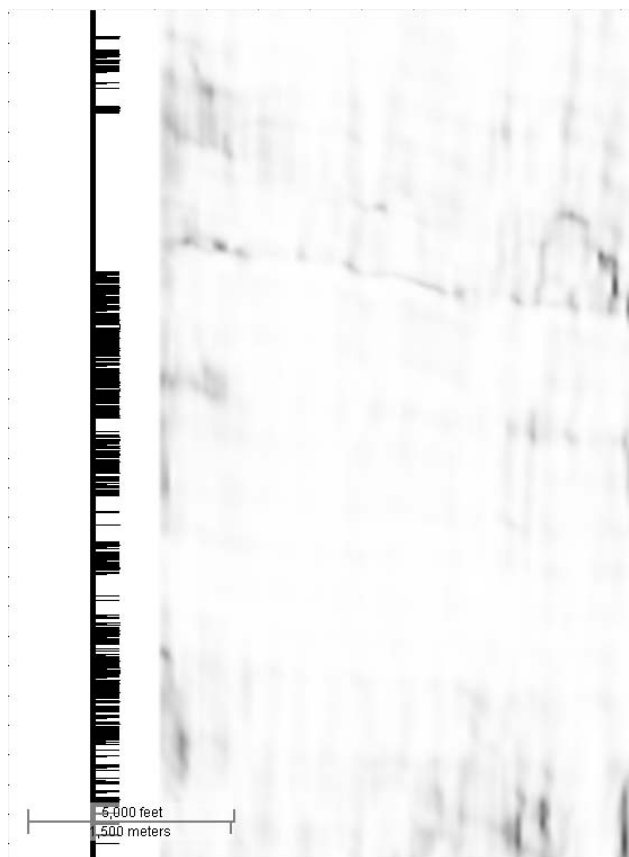


Figure 10 - Example well with a fracture likelihood curve calibrated to an image log to the left of the discontinuity volume.

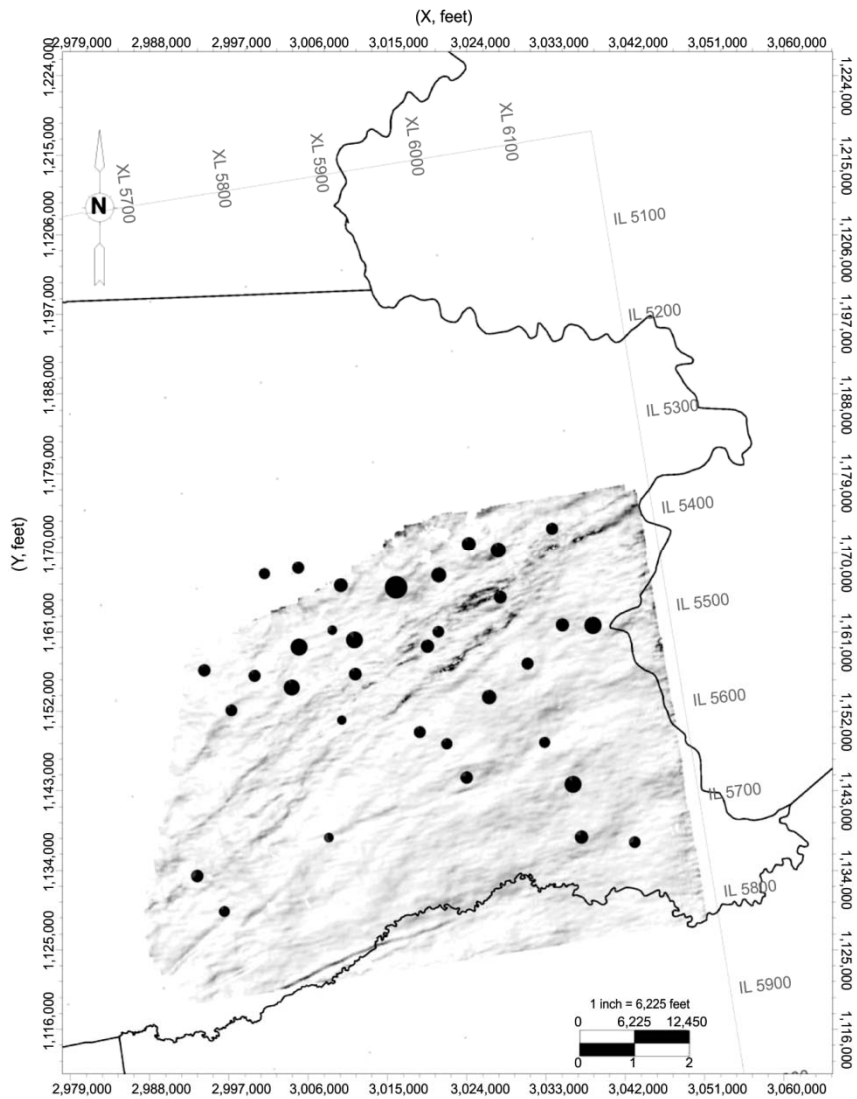


Figure 11 - Discontinuity slice through the Buda horizon with 90-day production bubble charts displayed for each well.

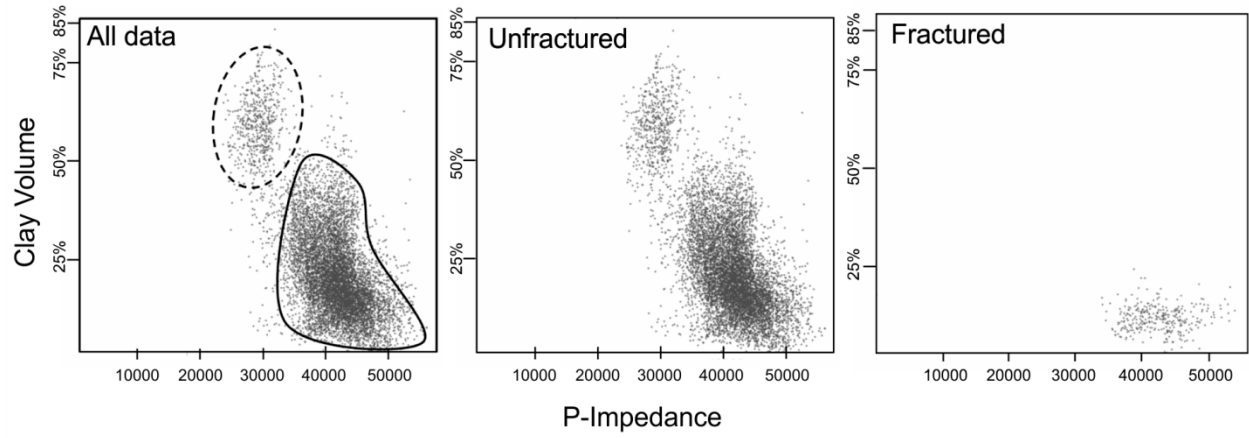


Figure 12 - Clay volume vs. P-impedance for the entire dataset, the unfractured dataset, and the fractured dataset. The high clay group is outlined by a dotted line, and the low clay group is outlined with a solid line.